

Shell model study of high-spin states and band terminations in ^{67}As

Vikas Kumar^{1,*} and Praveen C. Srivastava^{2,†}

¹*Department of Physics, Central University of Kashmir, Ganderbal 191 201, India*

²*Department of Physics, Indian Institute of Technology, Roorkee 247 667, India*

(Dated: April 27, 2020)

In the present work, recently available experimental data for different bands of ^{67}As [R. Wadsworth *et al.*, Phys. Rev. C **98**, 024313 (2018)] have been interpreted within the framework of the shell model in full $f_{5/2}pg_{9/2}$ model space using JUN45 and jj44b effective interactions. We have also reported the electromagnetic transition probabilities, quadrupole and magnetic moments of ^{67}As . The wave functions, particularly, the specific proton and neutron configurations that are involved to generate the total angular momentum are discussed for selected energy states of ^{67}As . The states $29/2^+$ - $45/2^+$ are described by three particles in $g_{9/2}$, while $47/2^+$ and $51/2^+$ states are described by five particles in $g_{9/2}$. The nine tentative states such as $41/2_1^+$ and $45/2_1^+$ in band-1b; $41/2_2^+$ and $45/2_2^+$ in band-1a; $43/2_2^+$, $47/2_2^+$ and $51/2_1^+$ in band-2a; $43/2_1^+$ and $47/2_1^+$ in band-2b are confirmed by the shell model. The variation of $E - E_{rot}$ energy versus spin for different bands is also shown to obtain useful information about band termination.

PACS numbers: 21.60.Cs, 21.60.Ev, 27.50.+e

I. INTRODUCTION

The band termination and nontermination is important properties of nuclei in the $Z, N = 28 - 50$ region. When we have few valence nucleons outside the ^{56}Ni core then nuclei exhibit band termination, while if valence nucleons are large then we have band nontermination. The experimental observation of band termination in non collective states of ^{62}Zn (6 valence

* vikasphysicsiitr@gmail.com

† praveen.srivastava@ph.iitr.ac.in

nucleons) is reported in Ref. [1]. The evidence for nontermination of rotational bands is observed in ^{74}Kr (18 valence nucleons) [2]. The nontermination of yrast bands at maximum configuration spin in ^{73}Kr is reported in Ref. [3]. Thus, the nontermination is important phenomenon for nuclei approaching the middle of the $Z, N = 28 - 50$ region [3]. The experimental evidence of band termination in ^{73}Br is reported in Ref. [4]. The band termination in ^{69}As is reported in Ref. [5].

In the more recent study of ^{67}As having 11 nucleons outside ^{56}Ni core exhibit band terminating structure [6]. The energy levels and γ -ray decay scheme of ^{67}As have been studied in Ref. [6] using the $^{40}\text{Ca}(^{36}\text{Ar}, 2\alpha p)^{67}\text{As}$ reaction at Argonne National Laboratory. In this work, two new band structures have been reported and further, these two bands are connected to the previously known energy levels [7]. The comparison of the experimental results for these two bands with theory using cranked Nilsson-Strutinsky model is reported in Ref. [6], both theory and experiments suggest that these structures can be interpreted in terms of configurations that involve three $g_{9/2}$ particles [6].

The study of these newly populated terminating bands in ^{67}As [6] using state-of-art large scale shell model calculations is very important. In this work, we have done a comprehensive shell model study corresponding to different bands within $f_{5/2}pg_{9/2}$ model space using two different jj44b and JUN45 interactions. Also, we have reported the electromagnetic transition probabilities, quadrupole and magnetic moments. In this region, the rotational features of $N = Z$ nuclei that possess large triaxiality because of shell effect are reported in Ref. [8]. For high-spin states recently we have done extensive shell model calculations in this region [9–18]. Thus shell model study of ^{67}As using these effective interactions is very crucial.

This paper is organized as follows: details about shell model calculations are given in section II. In section III, results and discussions are discussed. The decomposition of the total wave function is discussed in section IV. In section V, the electromagnetic properties are discussed. Finally, summary is drawn in section VI.

II. SHELL MODEL HAMILTONIAN

In the present shell model calculations, ^{56}Ni is taken as an inert core with the spherical orbits $1p_{3/2}$, $0f_{5/2}$, $1p_{1/2}$ and $0g_{9/2}$ in the model space for both neutrons and protons. For calculations, we used JUN45 and jj44b interactions. Brown and Lisetskiy developed the

jj44b interaction [19] and further this interaction was fitted with 600 experimental binding energies and excitation energies of nuclei with $Z = 28 - 30$ and $N = 48 - 50$ available in this region. Here, 30 linear combinations of JT coupled two-body matrix elements (TBME) are varied giving the rms deviation of about 250 keV from experimental data. The single particle energies (spe) are taken to be -9.6566, -9.2859, -8.2695 and -5.8944 MeV for the $1p_{3/2}$, $0f_{5/2}$, $1p_{1/2}$ and $0g_{9/2}$ orbits respectively [19]. The JUN45 [20] interaction is based on Bonn-C potential, the single-particle energies and two-body matrix elements were modified empirically with $A = 63 \sim 69$ mass region. The single-particle energies for the $1p_{3/2}$, $0f_{5/2}$, $1p_{1/2}$ and $0g_{9/2}$ orbitals are -9.828, -8.709, -7.839, and -6.262 MeV, respectively. The shell model calculations were performed using the shell model codes NuShellX [21], Antoine [22] and KSHELL [23].

III. RESULTS AND DISCUSSIONS

The comparison of calculated and experimental spectra for different bands of ^{67}As nucleus is given in Fig. 1 and Fig. 2 using JUN45 and jj44b effective interactions, respectively. In this paper, we have calculated many eigenvalues corresponding to each J^π and then we have classified into different bands on the basis of dominant $E2$ transitions between them. In order to identify the band structures, we have connected the states with a strong transition matrix elements between them and with similar configuration in the wave functions. The occupancies of the protons and neutrons in the orbits for the levels in various bands are given in Table I, and Table II corresponding to JUN45 and jj44b effective interactions, respectively.

A. Band-1

Several new high-spin positive parity states up to the excitation energy 15.876 MeV are well produced by the shell model calculations in band-1a and band-1b. All the sequences of the energy levels from both the shell model calculations are exactly matched with the experiments in this band. The calculated energy levels are slightly higher than the experiments this maybe because of the incompleteness of the basis state. The energy differences between $33/2^+ \rightarrow 29/2^+$ transition are observed 1604 [6] and 1081 keV [24] in the experiments, whereas in the present work this energy differences are 875 and 1873 keV using JUN45 and

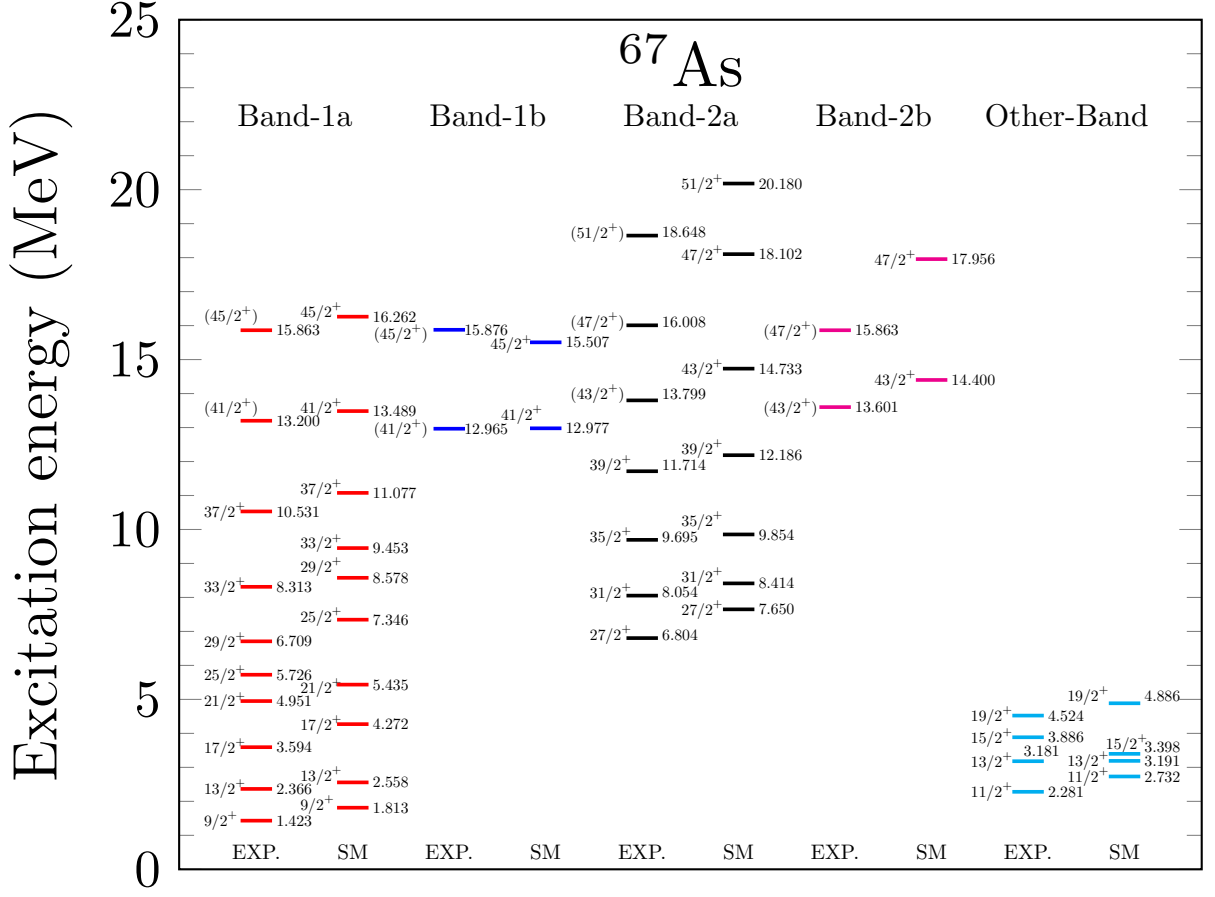


FIG. 1. Comparison of shell model results with experimental data for different bands with JUN45 interaction. The band numbers in the figure are as per the convention used in the experimental paper [6].

jj44b interactions, respectively.

In band-1a, the first two states $9/2^+$ and $13/2^+$ are lower by 464 and 186 keV than experiment in jj44b, while 390 and 192 keV higher than experiment in JUN45. The positive parity energy states $17/2^+$, $21/2^+$, $25/2^+$, $29/2^+$, $33/2^+$, $37/2^+$, $41/2^+$, and $45/2^+$ are 678, 484, 1620, 1869, 1140, 546, 289, and 399 keV higher in JUN45; while 177, 550, 137, 386, 655, 653, 699, and 1332 keV higher in jj44b. Both interactions predict $\pi(p_{3/2}^2, f_{5/2}^2, g_{9/2}^1) \otimes \nu(p_{3/2}^2, f_{5/2}^2, g_{9/2}^2)$ configuration for $9/2^+$ and $13/2^+$ states. In band-1b, the JUN45 prediction is very good for $41/2^+$ with a difference of only 12 keV with the experiment data, while this difference is 741 keV in jj44b. The $45/2^+$ state is lower by 369 keV in JUN45 while 529 keV higher in jj44b.

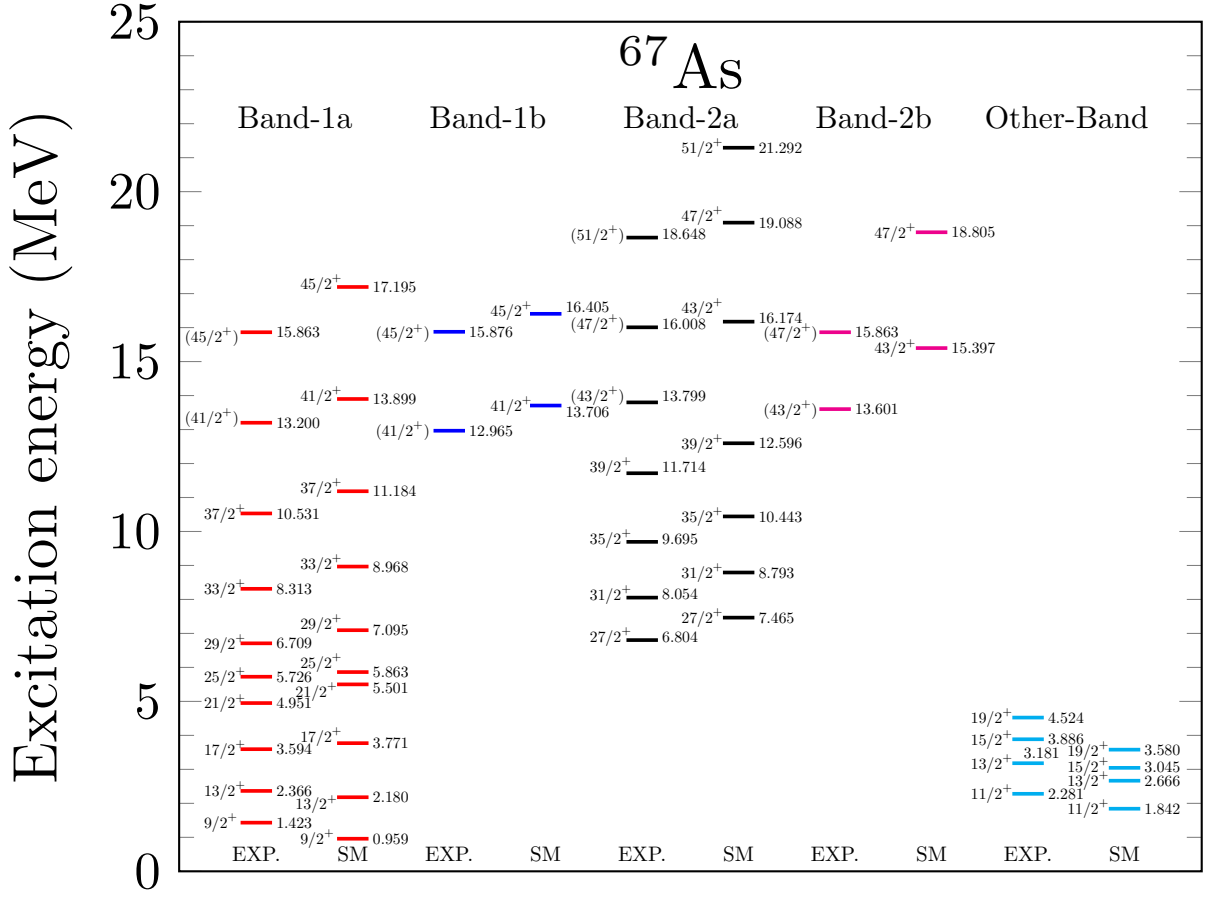


FIG. 2. Comparison of shell model results with experimental data for different bands with jj44b interaction. The band numbers in the figure are as per the convention used in the experimental paper [6].

There are two tentative spins $45/2_1^+$ and $45/2_2^+$ observed (band-1a and band-1b) in this experiment these tentative spins are confirmed by the shell model. A maximum spin of at least $49/2^+$ can be achieved with contributions from three particles in $g_{9/2}$ orbit reported in Ref. [6] using configuration-dependent cranked Nilsson-Strutinsky (CNS) approach [25–27] with Nilsson potential parameters [26]. The shell model configuration corresponding to positive-parity spin $45/2^+$ in band-1a and band-1b is $\pi(pf)_6^4(g_{9/2})_{4.5}^1\nu(pf)_6^4(g_{9/2})_8^2$, where (pf) refers to the $p_{3/2}$, $f_{5/2}$ and $p_{1/2}$ orbits, the upper number represents the number of particles in the specified orbits and the lower number represents the maximum spin contribution from particles in these orbits, this configuration also suggests that three particles are required in $g_{9/2}$ orbital to achieve $I_{max} = 45/2^+$ spin in this band. The single-particle energy of the $p_{1/2}$

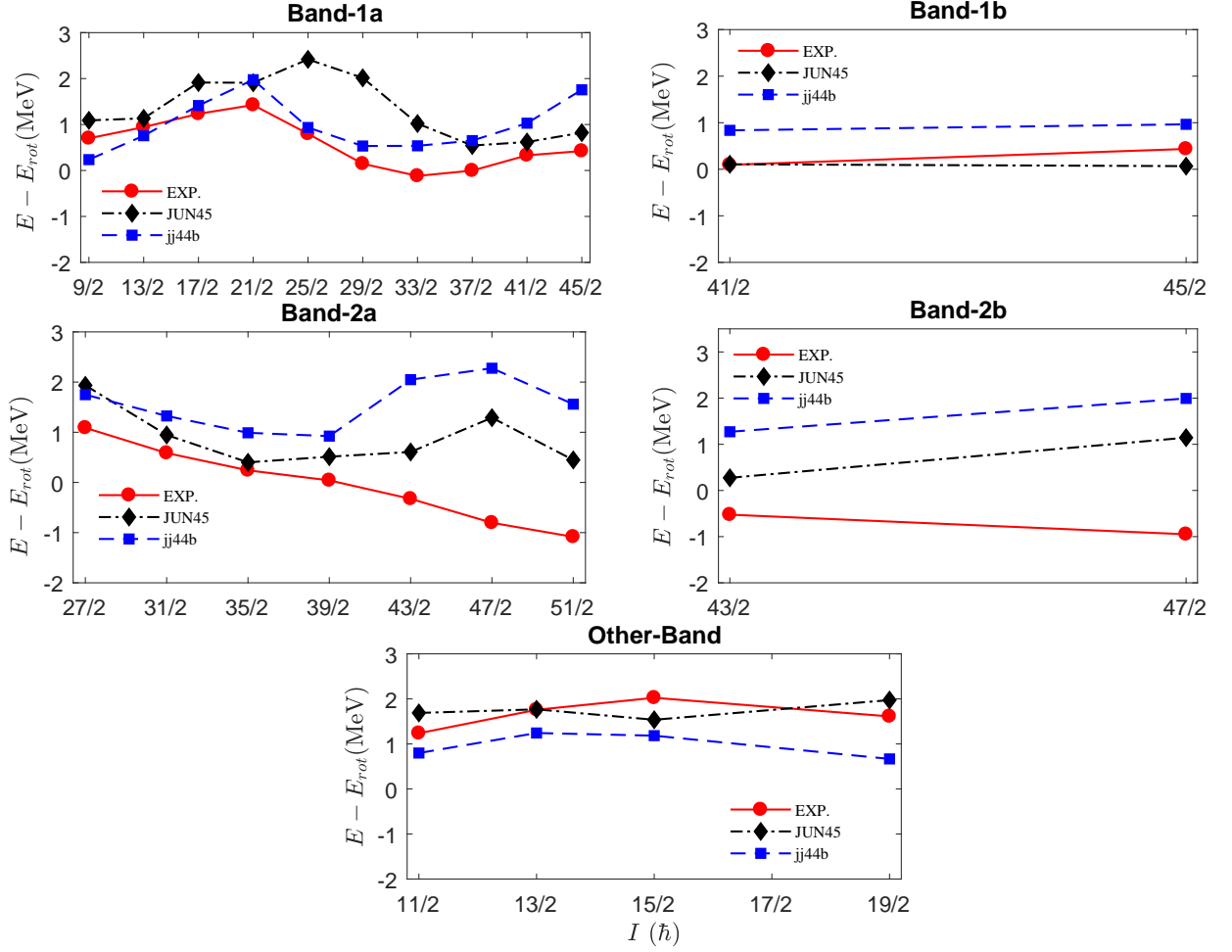


FIG. 3. Calculated and experimental energies corresponding to different bands in ^{67}As . A rotational reference $E_{rot} = 0.0292I(I + 1)$ has been subtracted.

orbit is lower in energy than $g_{9/2}$, but from the nucleon occupation table (Table I, and Table II) it is clear that $p_{1/2}$ orbit contributes little to the configuration.

B. Band-2

The spin sequence of the calculated positive parity energy levels in band-2a is the same as in the experiment. However, the energy levels $27/2^+$, $31/2^+$, $35/2^+$, $39/2^+$, $43/2^+$, $47/2^+$, and $51/2^+$ are 846, 360, 159, 472, 934, 2094, and 1532 keV higher in JUN45; while 661, 739, 748, 882, 2375, 3080, and 2644 keV higher in jj44b. In band-2b, the JUN45 results for the energy states $43/2^+$ and $47/2^+$ are 799 and 2093 keV higher; while 1796 and 2942 keV higher in jj44b. Overall the energy spectrum using JUN45 interaction are more closer to the

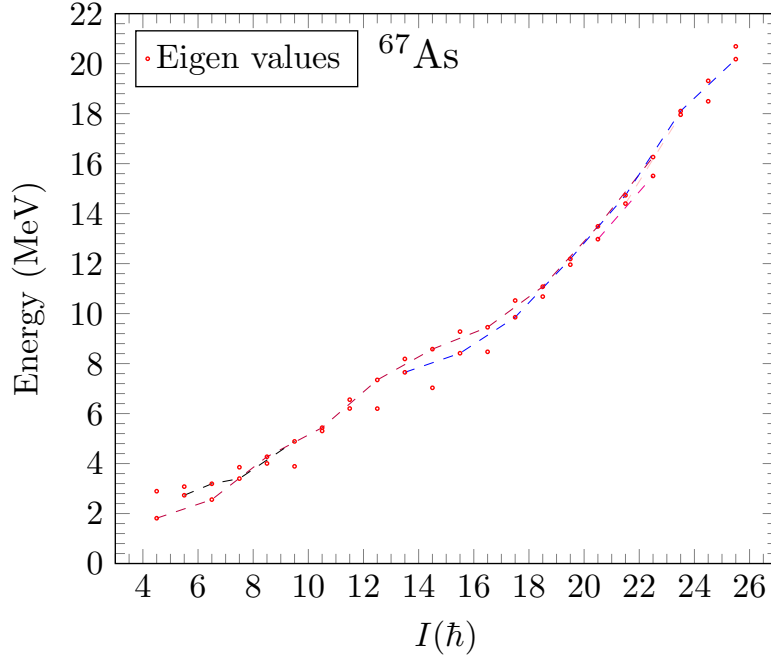


FIG. 4. Shell model predictions for different band in ^{67}As with JUN45 interaction.

experimental data. In the band-2a, the $27/2^+$ - $31/2^+$ - $35/2^+$ - $39/2^+$ - $43/2^+$ - $47/2^+$ states are due to three $g_{9/2}$ particles, while in band-2b, $47/2^+$ state is due to five $g_{9/2}$ particles.

The tentative spin ($51/2^+$) observed in the experiment is also confirmed by the shell model calculations. The shell model result supports the CNS prediction that such high-spin positive-parity states can only be formed in configuration involve five $g_{9/2}$ particles. The shell model configuration corresponding to positive-parity spin $51/2^+$ in band-2a is $\pi(pf)_{4.5}^3(g_{9/2})_4^2\nu(pf)_{4.5}^3(g_{9/2})_{8.5}^3$. From the analysis of configuration, it is clear that only three $g_{9/2}$ particles are involved in the configuration for the positive-parity band at low energy. From the nucleon occupation Table (Table I, and Table II), the $p_{1/2}$ orbit has little contribution to the configuration, although its single-particle energy is lower. As reported in Ref. [6] that all transitions in band 2 are most likely not stretched $B(E2)$ s because for example the lowest $51/2^+$ state (with five $g_{9/2}$ particles) is calculated at a much higher energy. This is supported by our shell model calculations here the difference between calculations and experiment becomes much larger for the $47/2^+$ and $51/2^+$ states in band 2.

C. Other-Band

The positive parity energy states $11/2^+$, $13/2^+$, $15/2^+$, and $19/2^+$ at 2281, 3181, 3886, and 4524 keV in Fig. 1 of Ref. [6] is defined as other band in the present work. These energy levels are successfully produced using both the shell model calculations. The sequence of the energy states in the experiment are exactly matched with the SM calculations. The configuration for different energy states in this band indicate that one particle is required in $g_{9/2}$ orbital to produce these spins and parity.

D. Variation of $E - E_{rot}$ energy with spin for different bands

Calculated and experimental energies for the different bands are shown in Fig. 3. For convenience a rotational reference has been subtracted. It is seen how the rotational behavior and band termination, are reasonably described by the shell model calculations. The related energies of the band members as expressed by $E - E_{rot}$ form a specific configuration dependent curve as a function of spin. The value of $E - E_{rot}$ become a minimum followed by a sharp increase before terminates. The kink in the curve is observed because of configuration changes. The JUN45 interaction is showing similar trend as in the experimental data for band-1a.

To identify the band structure, we have connected states with strong transitions matrix elements by lines as shown in Fig. 4. Also, these states are connected with similar dominant configuration in the wave functions.

IV. DECOMPOSITION OF TOTAL WAVE FUNCTION

From the analysis of the wave functions, it is possible to identify which nucleon pairs are broken to obtain the total angular momentum of the calculated states. The two components for neutrons and protons are I_n and I_p , respectively. These components are coupled to give the total angular momentum of each state. The decomposition of the total angular momentum of different band heads of ^{67}As nucleus into their $I_n \otimes I_p$ components using JUN45 interaction is given in Fig. 5. The percentage above 10% is written inside the squares, drawn with an area proportional to it. Percentage below 5% is not written.

The band head of band-1a is $9/2_1^+$, the dominant component (18%) of $9/2_1^+$ state at 1813

keV comes from fifth valance proton in $g_{9/2}$ orbital (thus total protons contribution, $I_p = 9/2$), while all the six neutrons are paired ($I_n = 0$). Other dominant component (20%) of this state comes from the neutrons paired ($I_n = 2$), and the fifth valance proton is contributing ($I_p = 9/2$). The dominant component (49%) of $41/2_1^+$ state (band head of band-1b) at 12977 keV come from the paired neutrons ($I_n = 12$), and the protons contributed ($I_p = 17/2$). Both the proton and neutron components are contributing to the state $41/2_1^+$, thus this state is a collective state. The $27/2_1^+$ state (the band head of band-2a) at 7650 keV has dominant component (18%) due to neutron are paired ($I_n = 9$), the protons contributed ($I_p = 9/2$). In similar way, we can explain the remaining band heads of ^{67}As . The states $43/2_1^+$ at 14400 keV and $11/2_1^+$ at 2732 keV are due to contribution from both neutrons and protons component thus these states are a collective states.

V. ELECTROMAGNETIC PROPERTIES

In Table III and IV, we have reported calculated $B(E2)$ values for different transitions in different bands using JUN45 and jj44b effective interactions, respectively. The calculated bands are well connected with larger $B(E2)$ values. However, in our calculation for band-1a with JUN45, the $B(E2; 29/2_2^+ \rightarrow 25/2_2^+)$ is very small. This is because there is a drastic change in the $g_{9/2}$ occupancy between $29/2_2^+$ and $25/2_2^+$ levels. Shell model predicts the structure of the $29/2_2^+$ level to be quite different from that of the other levels lying below. Similarly, in the case of jj44b, for band-1a, the $B(E2; 25/2_2^+ \rightarrow 21/2_2^+)$ is very small. This is because there is a drastic change in the $g_{9/2}$ occupancy between $25/2_2^+$ and $21/2_2^+$ levels. For the calculation of magnetic moments in the present work, we have used $g_s^{\text{eff}} = g_s^{\text{free}}$. The results of electric quadrupole and magnetic moments are listed in Table V for different bands using JUN45 and jj44b effective interactions. The calculated results from both the calculations are in a good agreement with each other. These predicted results might be very useful to compare upcoming experimental data.

TABLE I. Shell model results for configuration and occupancies of different states for ^{67}As using JUN45 interaction.

State	Configuration	nucleon occupation numbers $n_{ij}^\pi = (p_{3/2}, f_{5/2}, p_{1/2}, g_{9/2}), n_{ij}^\nu = (p_{3/2}, f_{5/2}, p_{1/2}, g_{9/2})$
Band-1a		
$9/2_1^+$	$\pi(p_{3/2}^2, f_{5/2}^2, p_{1/2}^0, g_{9/2}^1) \otimes \nu(p_{3/2}^2, f_{5/2}^2, p_{1/2}^0, g_{9/2}^2)$	(1.877, 1.681, 0.537, 0.905)(2.033, 2.092, 0.635, 1.240)
$13/2_1^+$	$\pi(p_{3/2}^2, f_{5/2}^2, p_{1/2}^0, g_{9/2}^1) \otimes \nu(p_{3/2}^2, f_{5/2}^2, p_{1/2}^0, g_{9/2}^2)$	(1.900, 1.750, 0.505, 0.845)(2.176, 1.957, 0.725, 1.141)
$17/2_2^+$	$\pi(p_{3/2}^2, f_{5/2}^3, p_{1/2}^0, g_{9/2}^0) \otimes \nu(p_{3/2}^2, f_{5/2}^3, p_{1/2}^1, g_{9/2}^1)$	(1.984, 1.831, 0.479, 0.706)(2.292, 1.899, 0.728, 1.081)
$21/2_2^+$	$\pi(p_{3/2}^2, f_{5/2}^3, p_{1/2}^0, g_{9/2}^0) \otimes \nu(p_{3/2}^2, f_{5/2}^3, p_{1/2}^0, g_{9/2}^1)$	(2.005, 1.942, 0.491, 0.562)(2.287, 2.274, 0.551, 0.888)
$25/2_2^+$	$\pi(p_{3/2}^2, f_{5/2}^2, p_{1/2}^0, g_{9/2}^1) \otimes \nu(p_{3/2}^2, f_{5/2}^3, p_{1/2}^1, g_{9/2}^0)$	(2.042, 1.984, 0.470, 0.503)(2.284, 2.323, 0.542, 0.852)
$29/2_2^+$	$\pi(p_{3/2}^2, f_{5/2}^2, p_{1/2}^0, g_{9/2}^1) \otimes \nu(p_{3/2}^2, f_{5/2}^2, p_{1/2}^0, g_{9/2}^2)$	(1.473, 1.541, 0.449, 1.537)(1.769, 2.191, 0.430, 1.610)
$33/2_2^+$	$\pi(p_{3/2}^2, f_{5/2}^1, p_{1/2}^0, g_{9/2}^2) \otimes \nu(p_{3/2}^2, f_{5/2}^3, p_{1/2}^0, g_{9/2}^1)$	(1.485, 1.504, 0.444, 1.568)(1.723, 2.283, 0.426, 1.569)
$37/2_2^+$	$\pi(p_{3/2}^2, f_{5/2}^2, p_{1/2}^0, g_{9/2}^1) \otimes \nu(p_{3/2}^2, f_{5/2}^2, p_{1/2}^0, g_{9/2}^2)$	(1.687, 1.818, 0.401, 1.095)(1.778, 1.820, 0.393, 2.008)
$41/2_2^+$	$\pi(p_{3/2}^2, f_{5/2}^2, p_{1/2}^0, g_{9/2}^1) \otimes \nu(p_{3/2}^2, f_{5/2}^2, p_{1/2}^0, g_{9/2}^2)$	(1.635, 1.897, 0.384, 1.084)(1.722, 1.849, 0.387, 2.042)
$45/2_2^+$	$\pi(p_{3/2}^2, f_{5/2}^2, p_{1/2}^0, g_{9/2}^1) \otimes \nu(p_{3/2}^1, f_{5/2}^2, p_{1/2}^1, g_{9/2}^2)$	(1.472, 2.072, 0.392, 1.064)(1.464, 2.075, 0.435, 2.025)
Band-1b		
$41/2_1^+$	$\pi(p_{3/2}^2, f_{5/2}^2, p_{1/2}^0, g_{9/2}^1) \otimes \nu(p_{3/2}^2, f_{5/2}^2, p_{1/2}^0, g_{9/2}^2)$	(1.719, 1.842, 0.350, 1.089)(1.761, 1.848, 0.362, 2.030)
$45/2_1^+$	$\pi(p_{3/2}^2, f_{5/2}^2, p_{1/2}^0, g_{9/2}^1) \otimes \nu(p_{3/2}^2, f_{5/2}^2, p_{1/2}^0, g_{9/2}^2)$	(1.704, 2.050, 0.142, 1.104)(1.809, 2.000, 0.156, 2.034)
Band-2a		
$27/2_1^+$	$\pi(p_{3/2}^2, f_{5/2}^2, p_{1/2}^0, g_{9/2}^1) \otimes \nu(p_{3/2}^2, f_{5/2}^2, p_{1/2}^0, g_{9/2}^2)$	(1.527, 1.958, 0.439, 1.076)(1.576, 1.947, 0.442, 2.035)
$31/2_1^+$	$\pi(p_{3/2}^2, f_{5/2}^2, p_{1/2}^0, g_{9/2}^1) \otimes \nu(p_{3/2}^2, f_{5/2}^2, p_{1/2}^0, g_{9/2}^2)$	(1.603, 1.886, 0.428, 1.083)(1.676, 1.856, 0.438, 2.030)
$35/2_1^+$	$\pi(p_{3/2}^2, f_{5/2}^2, p_{1/2}^0, g_{9/2}^1) \otimes \nu(p_{3/2}^2, f_{5/2}^2, p_{1/2}^0, g_{9/2}^2)$	(1.678, 1.782, 0.442, 1.097)(1.751, 1.770, 0.472, 2.007)
$39/2_2^+$	$\pi(p_{3/2}^2, f_{5/2}^2, p_{1/2}^0, g_{9/2}^1) \otimes \nu(p_{3/2}^2, f_{5/2}^2, p_{1/2}^0, g_{9/2}^2)$	(1.681, 1.820, 0.392, 1.107)(1.757, 1.780, 0.466, 1.996)
$43/2_2^+$	$\pi(p_{3/2}^2, f_{5/2}^1, p_{1/2}^0, g_{9/2}^2) \otimes \nu(p_{3/2}^2, f_{5/2}^2, p_{1/2}^1, g_{9/2}^1)$	(1.573, 1.420, 0.335, 1.671) (1.816, 2.252, 0.509, 1.423)
$47/2_2^+$	$\pi(p_{3/2}^2, f_{5/2}^2, p_{1/2}^0, g_{9/2}^1) \otimes \nu(p_{3/2}^2, f_{5/2}^1, p_{1/2}^1, g_{9/2}^2)$	(1.639, 2.030, 0.247, 1.083)(1.661, 1.955, 0.403, 1.981)
$51/2_1^+$	$\pi(p_{3/2}^2, f_{5/2}^1, p_{1/2}^0, g_{9/2}^2) \otimes \nu(p_{3/2}^2, f_{5/2}^1, p_{1/2}^0, g_{9/2}^3)$	(1.028, 1.573, 0.375, 2.024)(1.126, 1.514, 0.360, 3.000)
Band-2b		
$43/2_1^+$	$\pi(p_{3/2}^2, f_{5/2}^2, p_{1/2}^0, g_{9/2}^1) \otimes \nu(p_{3/2}^2, f_{5/2}^2, p_{1/2}^0, g_{9/2}^2)$	(1.706, 1.893, 0.323, 1.077) (1.800, 1.868, 0.326, 2.006)
$47/2_1^+$	$\pi(p_{3/2}^2, f_{5/2}^1, p_{1/2}^0, g_{9/2}^2) \otimes \nu(p_{3/2}^2, f_{5/2}^1, p_{1/2}^0, g_{9/2}^3)$	(1.298, 1.310, 0.374, 2.018) (1.328, 1.294, 0.372, 3.006)
Other Band		
$11/2_1^+$	$\pi(p_{3/2}^2, f_{5/2}^2, p_{1/2}^0, g_{9/2}^1) \otimes \nu(p_{3/2}^2, f_{5/2}^2, p_{1/2}^0, g_{9/2}^2)$	(1.822, 1.747, 0.543, 0.889)(1.977, 2.098, 0.639, 1.287)
$13/2_2^+$	$\pi(p_{3/2}^2, f_{5/2}^2, p_{1/2}^0, g_{9/2}^1) \otimes \nu(p_{3/2}^2, f_{5/2}^4, p_{1/2}^0, g_{9/2}^0)$	(1.963, 1.718, 0.542, 0.777) (2.272, 2.246, 0.592, 0.891)
$15/2_1^+$	$\pi(p_{3/2}^3, f_{5/2}^1, p_{1/2}^0, g_{9/2}^1) \otimes \nu(p_{3/2}^4, f_{5/2}^2, p_{1/2}^0, g_{9/2}^0)$	(2.069, 1.677, 0.452, 0.801)(2.322, 2.009, 0.650, 1.018)
$19/2_2^+$	$\pi(p_{3/2}^3, f_{5/2}^1, p_{1/2}^0, g_{9/2}^1) \otimes \nu(p_{3/2}^2, f_{5/2}^4, p_{1/2}^0, g_{9/2}^0)$	(2.158, 1.595, 0.552, 0.696)(2.316, 2.320, 0.554, 0.810)

TABLE II. Shell model results for configuration and occupancies of different states for ^{67}As using jj44b interaction.

State	Configuration	nucleon occupation numbers $n_{ij}^\pi = (p_{3/2}, f_{5/2}, p_{1/2}, g_{9/2}), n_{ij}^\nu = (p_{3/2}, f_{5/2}, p_{1/2}, g_{9/2})$
Band-1a		
$9/2_1^+$	$\pi(p_{3/2}^2, f_{5/2}^2, p_{1/2}^0, g_{9/2}^1) \otimes \nu(p_{3/2}^2, f_{5/2}^2, p_{1/2}^0, g_{9/2}^2)$	(1.855, 1.675, 0.514, 0.956)(2.116, 1.861, 0.676, 1.347)
$13/2_1^+$	$\pi(p_{3/2}^2, f_{5/2}^2, p_{1/2}^0, g_{9/2}^1) \otimes \nu(p_{3/2}^2, f_{5/2}^2, p_{1/2}^0, g_{9/2}^2)$	(1.924, 1.576, 0.558, 0.941)(2.060, 1.880, 0.639, 1.422)
$17/2_2^+$	$\pi(p_{3/2}^2, f_{5/2}^2, p_{1/2}^0, g_{9/2}^1) \otimes \nu(p_{3/2}^4, f_{5/2}^2, p_{1/2}^0, g_{9/2}^0)$	(1.989, 1.604, 0.563, 0.844)(2.426, 1.937, 0.574, 1.063)
$21/2_2^+$	$\pi(p_{3/2}^1, f_{5/2}^3, p_{1/2}^1, g_{9/2}^0) \otimes \nu(p_{3/2}^1, f_{5/2}^3, p_{1/2}^1, g_{9/2}^1)$	(1.746, 1.960, 0.676, 0.619)(2.037, 2.235, 0.697, 1.032)
$25/2_1^+$	$\pi(p_{3/2}^2, f_{5/2}^2, p_{1/2}^0, g_{9/2}^1) \otimes \nu(p_{3/2}^2, f_{5/2}^2, p_{1/2}^0, g_{9/2}^2)$	(2.019, 1.420, 0.482, 1.079)(2.013, 1.449, 0.494, 2.044)
$29/2_1^+$	$\pi(p_{3/2}^2, f_{5/2}^2, p_{1/2}^0, g_{9/2}^1) \otimes \nu(p_{3/2}^2, f_{5/2}^2, p_{1/2}^0, g_{9/2}^2)$	(1.946, 1.458, 0.525, 1.072)(1.933, 1.509, 0.514, 2.044)
$33/2_1^+$	$\pi(p_{3/2}^2, f_{5/2}^2, p_{1/2}^0, g_{9/2}^1) \otimes \nu(p_{3/2}^1, f_{5/2}^2, p_{1/2}^1, g_{9/2}^2)$	(1.723, 1.552, 0.626, 1.098)(1.724, 1.638, 0.633, 2.005)
$37/2_1^+$	$\pi(p_{3/2}^1, f_{5/2}^3, p_{1/2}^1, g_{9/2}^1) \otimes \nu(p_{3/2}^1, f_{5/2}^3, p_{1/2}^1, g_{9/2}^2)$	(1.433, 1.585, 0.684, 1.298)(1.824, 1.692, 0.686, 1.798)
$41/2_2^+$	$\pi(p_{3/2}^2, f_{5/2}^2, p_{1/2}^0, g_{9/2}^1) \otimes \nu(p_{3/2}^2, f_{5/2}^2, p_{1/2}^0, g_{9/2}^2)$	(1.628, 1.550, 0.573, 1.249)(1.889, 1.623, 0.643, 1.845)
$45/2_2^+$	$\pi(p_{3/2}^1, f_{5/2}^3, p_{1/2}^1, g_{9/2}^2) \otimes \nu(p_{3/2}^2, f_{5/2}^2, p_{1/2}^1, g_{9/2}^1)$	(1.251, 1.461, 0.600, 1.689)(1.945, 1.816, 0.843, 1.396)
Band-1b		
$41/2_1^+$	$\pi(p_{3/2}^2, f_{5/2}^2, p_{1/2}^0, g_{9/2}^1) \otimes \nu(p_{3/2}^2, f_{5/2}^2, p_{1/2}^0, g_{9/2}^2)$	(1.488, 1.677, 0.757, 1.079)(1.571, 1.698, 0.727, 2.005)
$45/2_1^+$	$\pi(p_{3/2}^2, f_{5/2}^2, p_{1/2}^0, g_{9/2}^1) \otimes \nu(p_{3/2}^2, f_{5/2}^2, p_{1/2}^0, g_{9/2}^2)$	(1.965, 1.532, 0.430, 1.073)(1.995, 1.500, 0.487, 2.018)
Band-2a		
$27/2_1^+$	$\pi(p_{3/2}^2, f_{5/2}^2, p_{1/2}^0, g_{9/2}^1) \otimes \nu(p_{3/2}^1, f_{5/2}^2, p_{1/2}^1, g_{9/2}^2)$	(1.687, 1.321, 0.489, 1.503)(1.899, 1.837, 0.607, 1.657)
$31/2_1^+$	$\pi(p_{3/2}^2, f_{5/2}^2, p_{1/2}^0, g_{9/2}^1) \otimes \nu(p_{3/2}^1, f_{5/2}^3, p_{1/2}^0, g_{9/2}^2)$	(1.660, 1.399, 0.552, 1.389)(1.698, 1.942, 0.622, 1.738)
$35/2_1^+$	$\pi(p_{3/2}^1, f_{5/2}^2, p_{1/2}^0, g_{9/2}^2) \otimes \nu(p_{3/2}^3, f_{5/2}^2, p_{1/2}^0, g_{9/2}^1)$	(1.366, 1.405, 0.589, 1.639)(1.890, 1.942, 0.643, 1.526)
$39/2_2^+$	$\pi(p_{3/2}^1, f_{5/2}^2, p_{1/2}^1, g_{9/2}^1) \otimes \nu(p_{3/2}^1, f_{5/2}^3, p_{1/2}^0, g_{9/2}^2)$	(1.270, 1.737, 0.784, 1.209)(1.291, 2.211, 0.627, 1.871)
$43/2_2^+$	$\pi(p_{3/2}^2, f_{5/2}^1, p_{1/2}^1, g_{9/2}^1) \otimes \nu(p_{3/2}^1, f_{5/2}^3, p_{1/2}^0, g_{9/2}^2)$	(1.641, 1.605, 0.597, 1.156)(1.633, 1.831, 0.605, 1.931)
$47/2_2^+$	$\pi(p_{3/2}^1, f_{5/2}^2, p_{1/2}^0, g_{9/2}^2) \otimes \nu(p_{3/2}^2, f_{5/2}^2, p_{1/2}^1, g_{9/2}^1)$	(1.508, 1.352, 0.532, 1.608)(2.248, 1.664, 0.584, 1.504)
$51/2_1^+$	$\pi(p_{3/2}^1, f_{5/2}^1, p_{1/2}^1, g_{9/2}^2) \otimes \nu(p_{3/2}^1, f_{5/2}^2, p_{1/2}^0, g_{9/2}^3)$	(1.232, 1.240, 0.513, 2.015)(1.269, 1.212, 0.519, 3.000)
Band-2b		
$43/2_1^+$	$\pi(p_{3/2}^1, f_{5/2}^2, p_{1/2}^0, g_{9/2}^2) \otimes \nu(p_{3/2}^3, f_{5/2}^2, p_{1/2}^0, g_{9/2}^1)$	(1.440, 1.452, 0.499, 1.609)(2.264, 1.677, 0.560, 1.499)
$47/2_1^+$	$\pi(p_{3/2}^1, f_{5/2}^2, p_{1/2}^0, g_{9/2}^2) \otimes \nu(p_{3/2}^1, f_{5/2}^2, p_{1/2}^0, g_{9/2}^3)$	(1.242, 1.209, 0.540, 2.009)(1.280, 1.215, 0.534, 2.971)
Other Band		
$11/2_1^+$	$\pi(p_{3/2}^1, f_{5/2}^2, p_{1/2}^1, g_{9/2}^1) \otimes \nu(p_{3/2}^2, f_{5/2}^3, p_{1/2}^1, g_{9/2}^0)$	(1.491, 1.869, 0.709, 0.930)(2.184, 2.089, 0.722, 1.005)
$13/2_2^+$	$\pi(p_{3/2}^2, f_{5/2}^2, p_{1/2}^0, g_{9/2}^1) \otimes \nu(p_{3/2}^4, f_{5/2}^2, p_{1/2}^0, g_{9/2}^0)$	(1.944, 1.649, 0.543, 0.864)(2.438, 1.950, 0.580, 1.032)
$15/2_1^+$	$\pi(p_{3/2}^1, f_{5/2}^3, p_{1/2}^0, g_{9/2}^1) \otimes \nu(p_{3/2}^2, f_{5/2}^2, p_{1/2}^2, g_{9/2}^0)$	(1.533, 2.009, 0.514, 0.943)(2.077, 2.186, 0.724, 1.013)
$19/2_2^+$	$\pi(p_{3/2}^3, f_{5/2}^2, p_{1/2}^0, g_{9/2}^0) \otimes \nu(p_{3/2}^3, f_{5/2}^2, p_{1/2}^0, g_{9/2}^1)$	(1.953, 1.876, 0.491, 0.680)(2.398, 1.898, 0.580, 1.124)

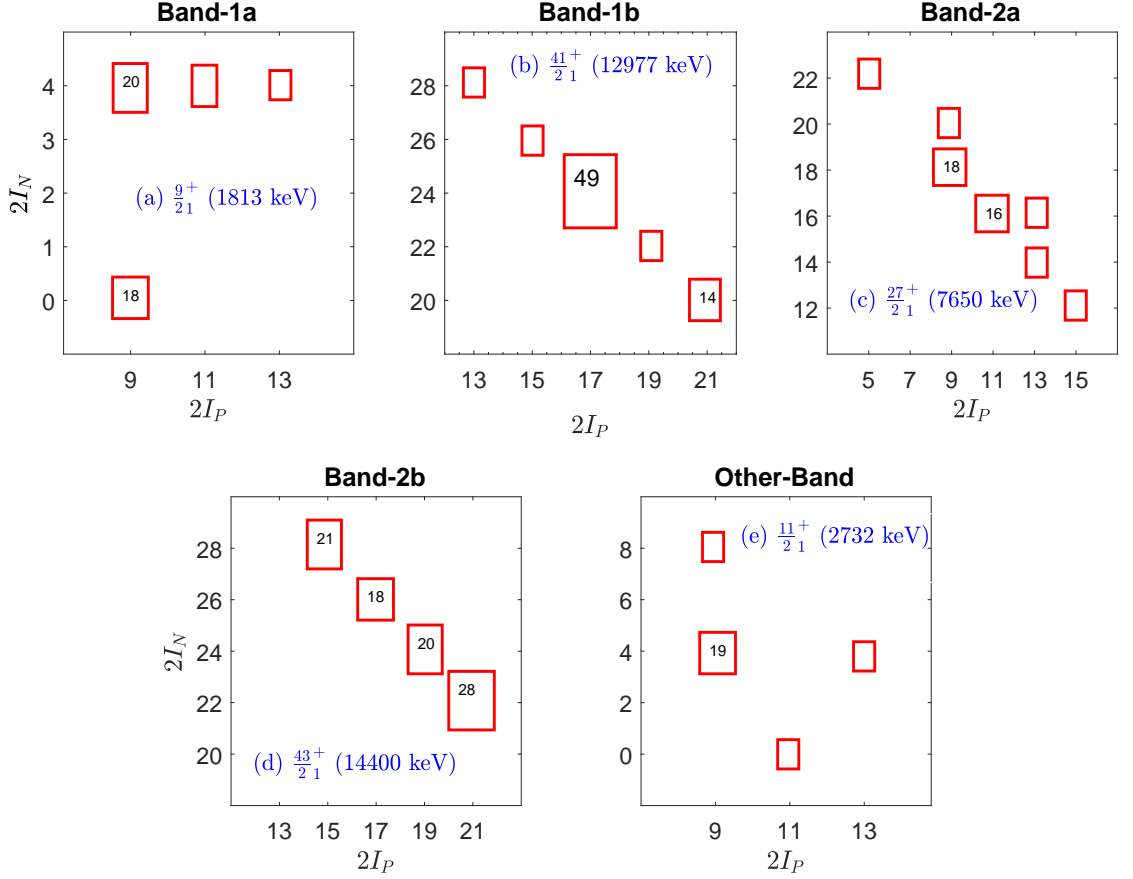


FIG. 5. Decomposition of the total angular momentum of different band heads of ^{67}As into their $I_n \otimes I_p$ components for JUN45 interaction. The percentage above 10% is written inside the squares, drawn with an area proportional to it. Percentage below 5% is not written.

VI. SUMMARY

Motivated by recent experimental data of different bands [6] for ^{67}As , we have reported the comprehensive shell model study of different bands in $f_{5/2}pg_{9/2}$ model space using JUN45 and jj44b effective interactions. The following broad conclusions are drawn:

- The high spin structures of negative and positive parity bands are successfully described by both the effective interactions for the full $f_{5/2}pg_{9/2}$ model space.
- Some tentative spins-parity high-energy states [6] such as $41/2_1^+$ and $45/2_1^+$ in band-1b; $41/2_2^+$ and $45/2_2^+$ in band-1a; $43/2_2^+$, $47/2_2^+$ and $51/2_1^+$ in band-2a; $43/2_1^+$ and $47/2_1^+$ in band-2b are confirmed by the shell model.

TABLE III. Calculated $B(E2)$ values (in $e^2 fm^4$) for ^{67}As using JUN45 interaction with $e_\pi = 1.5e$; $e_\nu = 0.5e$.

Transition	Band -1a	Transition	Band -2a
$B(E2; 13/2_1^+ \rightarrow 9/2_1^+)$	177	$B(E2; 31/2_1^+ \rightarrow 27/2_1^+)$	293
$B(E2; 17/2_2^+ \rightarrow 13/2_1^+)$	145	$B(E2; 35/2_1^+ \rightarrow 31/2_1^+)$	257
$B(E2; 21/2_2^+ \rightarrow 17/2_2^+)$	26	$B(E2; 39/2_2^+ \rightarrow 35/2_1^+)$	118
$B(E2; 25/2_2^+ \rightarrow 21/2_2^+)$	277	$B(E2; 43/2_2^+ \rightarrow 39/2_2^+)$	24
$B(E2; 29/2_2^+ \rightarrow 25/2_2^+)$	0.12	$B(E2; 47/2_2^+ \rightarrow 43/2_2^+)$	3
$B(E2; 33/2_2^+ \rightarrow 29/2_2^+)$	295	$B(E2; 51/2_1^+ \rightarrow 47/2_2^+)$	0.02
$B(E2; 37/2_2^+ \rightarrow 33/2_2^+)$	79		
$B(E2; 41/2_2^+ \rightarrow 37/2_2^+)$	164		
$B(E2; 45/2_2^+ \rightarrow 41/2_2^+)$	23		
Transition	Band -1b	Transition	Band -2b
$B(E2; 45/2_1^+ \rightarrow 41/2_1^+)$	113	$B(E2; 47/2_1^+ \rightarrow 43/2_1^+)$	0.002
Transition	Other Band		
$B(E2; 13/2_2^+ \rightarrow 11/2_1^+)$	90		
$B(E2; 15/2_1^+ \rightarrow 13/2_2^+)$	37		
$B(E2; 19/2_2^+ \rightarrow 15/2_1^+)$	169		

- All the newly observed states in band-1a, band-1b, band-2a, and band-2b are successfully described by the shell model calculations.
- The order of $11/2^+$ - $13/2^+$ - $15/2^+$ - $19/2^+$ states in other band is correctly reproduced by the shell model.
- The difference between shell model and experiment becomes much larger for the $47/2^+$ and $51/2^+$ states in band 2. Similar observation is also reported by the CNS calculations.
- The shell model result support the earlier work done using cranked Nilsson-Strutinsky calculations in Ref. [6] that the high-spin positive-parity states can only be formed in

TABLE IV. Calculated $B(E2)$ values (in $e^2 fm^4$) for ^{67}As using jj44b interaction with $e_\pi = 1.5e$; $e_\nu = 0.5e$.

Transition	Band -1a	Transition	Band -2a
$B(E2; 13/2_1^+ \rightarrow 9/2_1^+)$	237	$B(E2; 31/2_1^+ \rightarrow 27/2_1^+)$	236
$B(E2; 17/2_2^+ \rightarrow 13/2_1^+)$	167	$B(E2; 35/2_1^+ \rightarrow 31/2_1^+)$	104
$B(E2; 21/2_2^+ \rightarrow 17/2_2^+)$	198	$B(E2; 39/2_2^+ \rightarrow 35/2_1^+)$	8
$B(E2; 25/2_1^+ \rightarrow 21/2_2^+)$	2.48	$B(E2; 43/2_2^+ \rightarrow 39/2_2^+)$	20
$B(E2; 29/2_1^+ \rightarrow 25/2_1^+)$	309	$B(E2; 47/2_2^+ \rightarrow 43/2_2^+)$	3
$B(E2; 33/2_1^+ \rightarrow 29/2_1^+)$	250	$B(E2; 51/2_1^+ \rightarrow 47/2_2^+)$	5
$B(E2; 37/2_1^+ \rightarrow 33/2_1^+)$	170		
$B(E2; 41/2_2^+ \rightarrow 37/2_1^+)$	83		
$B(E2; 45/2_2^+ \rightarrow 41/2_2^+)$	43		
Transition	Band -1b	Transition	Band -2b
$B(E2; 45/2_1^+ \rightarrow 41/2_1^+)$	94	$B(E2; 47/2_1^+ \rightarrow 43/2_1^+)$	8
Transition	Other Band		
$B(E2; 13/2_2^+ \rightarrow 11/2_1^+)$	115		
$B(E2; 15/2_1^+ \rightarrow 13/2_2^+)$	24		
$B(E2; 19/2_2^+ \rightarrow 15/2_1^+)$	77		

configurations involving three $g_{9/2}$ particles for band-1 and five particles in $g_{9/2}$ orbit in band-2.

- High-spin states in ^{67}As nucleus come from breaking of neutron/proton pairs. The $41/2_1^+$ state is a collective state because both neutrons and protons pairs are responsible to generate this state.
- The $E - E_{rot}$ energy curve reflect the concept of configuration changes and band termination.
- Our predicted value of quadrupole and magnetic moments might be useful to compare the future experimental data.

TABLE V. The calculated electric quadrupole moments Q_s (in eb) and magnetic moments μ (in μ_N). The effective charges $e_p=1.5e$, $e_n=0.5e$ and $g_s^{\text{eff}} = g_s^{\text{free}}$ are used.

Band-1a				Band-2a			
		Electric Moments	Magnetic Moments			Electric Moments	Magnetic Moments
9/2 ⁺	Expt	N/A	N/A	27/2 ⁺	Expt	N/A	N/A
	JUN45	-0.642	+4.744		JUN45	-0.755	+4.150
	jj44b	-0.667	+4.805		jj44b	-0.943	+7.253
13/2 ⁺	Expt	N/A	N/A	31/2 ⁺	Expt	N/A	N/A
	JUN45	-0.787	+5.912		JUN45	-0.809	+5.100
	jj44b	-0.779	+5.995		jj44b	-0.954	+7.885
17/2 ⁺	Expt	N/A	N/A	35/2 ⁺	Expt	N/A	N/A
	JUN45	-0.762	+6.419		JUN45	-0.840	+6.270
	jj44b	-0.594	+5.096		jj44b	-0.922	+10.111
21/2 ⁺	Expt	N/A	N/A	39/2 ⁺	Expt	N/A	N/A
	JUN45	-0.536	+4.328		JUN45	-0.685	+7.254
	jj44b	-0.589	+3.645		jj44b	-0.877	+10.610
25/2 ⁺	Expt	N/A	N/A	43/2 ⁺	Expt	N/A	N/A
	JUN45	-0.543	+5.136		JUN45	-0.844	+11.284
	jj44b	-0.975	+3.694		jj44b	-0.811	+8.450
29/2 ⁺	Expt	N/A	N/A	47/2 ⁺	Expt	N/A	N/A
	JUN45	-0.844	+7.541		JUN45	-0.620	+9.566
	jj44b	-1.016	+4.625		jj44b	-0.870	+12.112
33/2 ⁺	Expt	N/A	N/A	51/2 ⁺	Expt	N/A	N/A
	JUN45	-0.879	+8.528		JUN45	-0.894	+11.055
	jj44b	-1.034	+5.827		jj44b	-0.978	+10.929
				Band -2b			
37/2 ⁺	Expt	N/A	N/A	43/2 ⁺	Expt	N/A	N/A
	JUN45	-0.371	+6.738		JUN45	-0.632	+8.411
	jj44b	-1.014	+8.229		jj44b	-0.867	+11.271
41/2 ⁺	Expt	N/A	N/A	47/2 ⁺	Expt	N/A	N/A
	JUN45	-0.660	+7.643		JUN45	-0.944	+9.886
	jj44b	-0.860	+8.665		jj44b	-0.954	+10.043
				Other Band			
45/2 ⁺	Expt	N/A	N/A	11/2 ⁺	Expt	N/A	N/A
	JUN45	-0.733	+8.385		JUN45	-0.369	+4.773
	jj44b	-0.960	+11.649		jj44b	-0.647	+3.128
Band-1b							
41/2 ⁺	Expt	N/A	N/A	13/2 ⁺	Expt	N/A	N/A
	JUN45	-0.649	+7.628		JUN45	-0.415	+4.118
	jj44b	-0.943	+7.706		jj44b	-0.450	+3.973
45/2 ⁺	Expt	N/A	N/A	15/2 ⁺	Expt	N/A	N/A
	JUN45	-0.572	+8.985		JUN45	-0.535	+5.600
	jj44b	-0.793	+8.387		jj44b	-0.708	+4.614
				19/2 ⁺	Expt	N/A	N/A
					JUN45	-0.573	+5.600
					jj44b	-0.523	+3.034

Thus, present comprehensive study will add more informations to earlier work [6].

ACKNOWLEDGMENTS

V.K. acknowledges financial support from SERB Project (File No. EEQ/2019/000084), Govt. of India. We acknowledge Prayag 5 nodes computational facility at Physics Department, IIT-Roorkee. We would like to thank Prof. I. Ragnarsson for useful discussions during this work.

-
- [1] C. E. Svensson *et al.*, “Smooth termination of rotational bands in ^{62}Zn : evidence for a loss of collectivity,” *Phys. Rev. Lett.* **80**, 2558 (1998).
 - [2] J. J. Valiente-Dobon *et al.*, “Evidence for nontermination of rotational bands in ^{74}Kr ,” *Phys. Rev. Lett.* **95**, 0232501 (2005).
 - [3] T. Steinhardt *et al.*, “Non-termination of yrast bands at maximum configuration spin in ^{73}Kr ,” *Phys. Rev. C* **81**, 054307 (2010).
 - [4] C. Plettner *et al.*, “Very high rotational frequencies and band termination in ^{73}Br ,” *Phys. Rev. C* **62**, 014313 (2000).
 - [5] I. Stefanescu *et al.*, “High-spin states and band terminations in ^{69}As ,” *Phys. Rev. C* **70**, 044304 (2004).
 - [6] R. Wadsworth *et al.*, “Terminating states in the positive-parity structures of ^{67}As ,” *Phys. Rev. C* **98**, 024313 (2018).
 - [7] R. Orlandi *et al.*, “Coherent contributions to isospin mixing in the mirror pair ^{67}As and ^{67}Se ,” *Phys. Rev. Lett.* **103**, 052501 (2009).
 - [8] P.C. Srivastava, S. Aberg and I. Ragnarsson, “Triaxial rotation-axis flip triggered by an isoscalar $n - p$ pair,” *Phys. Rev. C* **95**, 011303(R) (2017).
 - [9] P.C. Srivastava, R. Sahu and V.K.B. Kota, “Shell model results for $T = 1$ and $T = 0$ bands in ^{66}As ,” *J. Physics G: Nuclear and Particle Physics* **44**, 125107 (2017).
 - [10] P.C. Srivastava, “Structure of $^{71-78}\text{Ga}$ isotopes in the $f_{5/2}pg_{9/2}$ and $fp_{g_{9/2}}$ spaces,” *J. Phys. G: Nucl. Part. Phys.* **39**, 015102 (2012).

- [11] J.G. Hirsch and P.C. Srivastava, “Shell model description of Ge isotopes,” *J. Phys.: Conf. Ser.* **387**, 012020 (2012).
- [12] P. C. Srivastava and M. J. Ermamatov, “Comparison of shell model results for even-even Se isotopes,” *Phys. Scr.* **88**, 045201 (2013).
- [13] V. Kumar, P. C. Srivastava, Irving O. Morales, “High-spin structures of $^{77,79,81,83}\text{As}$ isotopes,” *Mod. Phys. Lett. A*, Vol. **30**, 1550093 (2015).
- [14] P. C. Srivastava, R. Sahu, and V. K. B. Kota, “Shell model and deformed shell model spectroscopy of ^{62}Ga ,” *Eur. Phys. J. A : Hadrons and Nuclei* **51**, 3 (2017).
- [15] S. Kumar, N. Kumar, S. Mandal, S.C. Pancholi, P.C. Srivastava, A.K. Jain et al., “High spin band structure of ^{85}Sr ,” *Phys. Rev. C* **90**, 024315 (2014).
- [16] N. Kumar, S. Kumar, V. Kumar, S.K. Mandal, R. Palit, S. Saha, J. Sethi, T. Trivedi, S.C. Pancholi, and P.C. Srivastava, “ Polarization measurements and high-spin states in ^{86}Sr ,” *Nucl. Phys. A* **955**, 1 (2016).
- [17] S. Saha, R. Palit, J. Sethi, S. Biswas, P. Singh, T. Trivedi, D. Choudhury, and P.C. Srivastava, “Investigation of the high spin structure of ^{88}Zr ,” *Phys. Rev. C* **89**, 044315 (2014).
- [18] P. Singh, R. Palit, S. Saha, J. Sethi, S. Biswas, D. Choudhury, P.C. Srivastava, and T. Trivedi, “Yrast structure of the shell model nucleus ^{89}Nb ,” *Phys. Rev. C* **90**, 014306 (2014).
- [19] B. Cheal *et al.*, “Nuclear spins and moments of Ga isotopes reveal sudden structural changes between $N = 40$ and $N = 50$,” *Phys. Rev. Lett.* **104**, 252502 (2010).
- [20] M. Honma, T. Otsuka, T. Mizusaki, and M. Hjorth-Jensen, “New effective interaction for f_5pg_9 -shell nuclei,” *Phys. Rev. C* **80**, 064323 (2009).
- [21] B. A. Brown and W. D. M. Rae, “The Shell-Model Code NuShellX@MSU”, *Nucl. Data Sheets* **120**, 115 (2014).
- [22] E. Caurier, G. Martínez-Pinedo, F. Nowacki, A. Poves, and A. P. Zuker, “The shell model as a unified view of nuclear structure,” *Rev. Mod. Phys.* **77**, 427 (2005).
- [23] N. Shimizu, T. Mizusaki, Y. Utsuno and Y. Tsunoda, “Thick-restart block Lanczos method for large-scale shell-model calculations,” *Comput. Phys. Comm.* **244**, 372 (2019).
- [24] D. G. Jenkins *et al.*, “Stability of oblate shapes in the vicinity of $N = Z = 34$ ^{68}Se : Bands in ^{69}Se and ^{67}As ,” *Phys. Rev. C* **64**, 064311 (2001).
- [25] A. V. Afanasjev, D. B. Fossan, G. J. Lane, and I. Ragnarsson, “Termination of rotational bands: disappearance of quantum many-body collectivity,” *Phys. Rep.* **322**, 1 (1999).

- [26] T. Bengtsson and I Ragnarsson, “Rotational bands and particle-hole excitations at very high spin,” *Nucl. Phys. A* **436**, 14 (1985).
- [27] B. G. Carlsson and I. Ragnarsson, “Calculating the nuclear mass in the very high angular momentum regime,” *Phys. Rev. C* **74**, 011302(R) (2006).